

Monte-Carlo Simulation of Electromigration in Polycrystalline Metal Stripes

Stefano Di Pascoli

Dipartimento di Ingegneria dell'Informazione: Elettronica, Informatica, Telecomunicazioni,
Università di Pisa

Giuseppe Iannaccone

Dipartimento di Ingegneria dell'Informazione: Elettronica, Informatica, Telecomunicazioni,
Università di Pisa

Monte Carlo simulation of electromigration in polycrystalline metal stripes

S Di Pascoli and G Iannaccone

Dipartimento di Ingegneria dell'Informazione: Elettronica, Informatica, Telecomunicazioni, Università degli studi di Pisa, Via Diotisalvi 2, I-56126 Pisa, Italy

E-mail: dipas@pimac2.iet.unipi.it

Received 31 August 1999, accepted for publication 31 March 2000

Abstract. We have developed a Monte Carlo simulator of the electromigration process in polycrystalline metal stripes. Stripes with different average grain size can be generated with Voronoi tessellation, and mapped onto a network of resistors. The proposed model includes the major role played by grain boundaries and by the current density redistribution within the stripe following void formation. Simulations of stripes with different grain sizes and different widths are shown, and a few expressions for the failure probability are compared on the basis of their capability of reproducing the experimental results. In addition, electromigration noise has been computed, recovering the characteristic $1/f^\gamma$ ($\gamma \approx 2$) behaviour. The substantial qualitative agreement between our calculations and the experimental results is a convincing test of the capability of the model proposed to include the relevant physics.

1. Introduction

The capability of modelling random defects and failures is emerging as a major issue in device and process modelling. Indeed, it could provide information significant from a statistical point of view on dispersion of device and circuit parameters and on reliability problems.

In this paper, we focus on the simulation of the electromigration process in polycrystalline metal lines, which is a major problem for the evolution of ULSI technology: as the widths of metal interconnects shrink and current densities increase, failures induced by electromigration can occur in relatively short times and reduce considerably the average circuit lifetime. Many efforts have been made to understand and control the electromigration process, by means of experiments [1–3] and theoretical modelling [4–7]. Experiments have allowed us to establish the major role played by atom diffusion along external surfaces and grain boundaries [1]. Gungor and Maroudas [7] have modelled generation of voids along the external surfaces and their successive propagation within a single grain in bamboo-like structures. We consider the case in which damage starts and evolves from grain boundaries, with the main objective of reproducing the resistance evolution of polycrystalline metal lines subjected to current stress. We have developed a Monte Carlo simulation code which takes into account both the polycrystalline nature of the metal line and the current density redistribution effect due to void enlargement. Even if this approach has sometimes appeared in the literature [4, 6], the main focus has been usually put on the mean time to failure, which is dominated by the random final catastrophic

failure and provides only partial information on the entire electromigration process. Instead, we simulated the complete evolution of the damage, in order to gather information on the whole process, and in particular on the initial phase, where the total resistance increases by only a few percent. Moreover, this approach permits us also to simulate the noise spectrum, which can be compared with the typical $1/f^\gamma$ noise which has been observed in many electromigration experiments [8].

2. Model

The simulations were performed on samples of polycrystalline metal films generated by means of a nucleation and growth algorithm [6] from which rectangular stripes of different dimensions were obtained. These polycrystalline stripes are discretized into a square lattice of uniformly spaced nodes, connected with resistors (as shown in figure 1).

Every crystal of the polycrystalline film is represented by a convex cluster of connected nodes. The resistors of the network have the same resistance and are divided into two classes: resistors connecting nodes in the same crystal grain ('bulk' resistors) and resistors crossing a grain boundary and connecting nodes from two adjacent grains ('boundary' resistors) which are represented with thin and thick lines in figure 1, respectively.

The stripes are then stressed with a constant current stimulus. The flow-chart of the simulation procedure is shown in figure 2. The main cycle consists of two phases: first, the total resistance of the network and the currents in each resistor are computed by solving the electrical problem

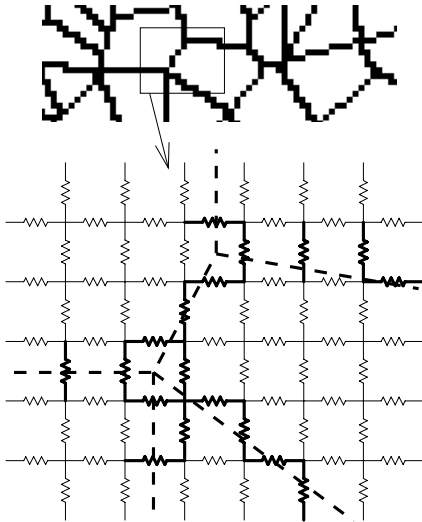


Figure 1. Grain structure (above) and corresponding resistor network (below). Thick-line resistors are those traversing grain boundaries ('boundary' resistors).

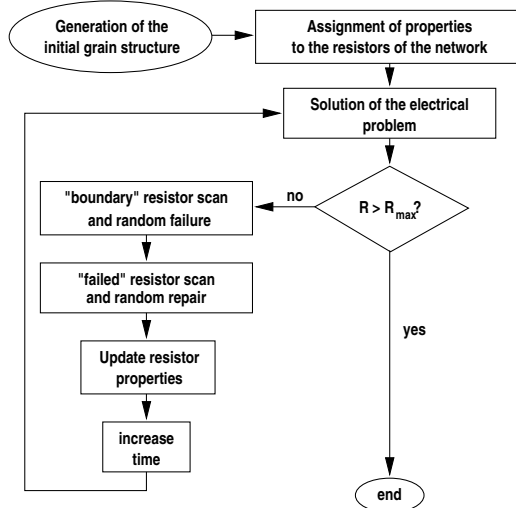


Figure 2. Flow-chart of the simulation program.

with a successive over-relaxation method with Chebishev acceleration [9]. In the second phase all the boundary resistors of the network are sequentially examined: the i th boundary resistor, in which flows a current I_i , has a failure probability given by:

$$P_{fi} = A(\exp(I_i/I_0) - 1) \quad (1)$$

where A and I_0 are constant during the simulation. Then, each failed resistor is considered and possibly repaired with a fixed probability P_r .

At the end of this phase, resistor properties are updated: failed resistors are removed from the network; resistors contacting a failed resistor become 'boundary' resistors; repaired resistors are re-inserted in the network as 'boundary' resistors. Then, as shown in figure 2, time is increased and the cycle is repeated, until the total resistance of the network becomes greater than a certain value.

The choice of the failure probability of equation (1) and of P_r is somewhat arbitrary, and based on phenomenological

arguments. First, we want to force damage to evolve along grain boundaries, therefore we allow only boundary resistors to fail; second, failures must be activated by current, since we need to introduce a positive feedback that leads to the abrupt failure of the whole stripe. The exponential law warrants that as a small region of the stripe is damaged, resistors close to that region experience a current increase which exponentially increases their failure probability, so that the damaged region typically grows at an accelerated rate until the stripe is open-circuited. A comparison of the effects of different choices of (1) is presented in section 3. The choice of P_r is based on the assumption that repairs are due to atom thermal diffusion and is consequently independent of current.

Although in an electromigration test the temperature of the stripe can be rather higher than that of the substrate and of the environment, the temperature gradient in the stripe itself is very small and consequently we have not included in the model the temperature dependence of the failure probability. The value of the parameter A is chosen in such a way that on average there is less than one failure per simulation cycle.

3. Results

The structure of the first stripe we consider is shown in figure 3: it is mapped onto a resistor network of 30×200 nodes, and grains have an average area of 400 nodes. The simulations have been performed with $I_{AV}/I_0 = 2$, where I_{AV} is the average current per longitudinal resistor and is therefore proportional to the stimulus current density. Each simulation is performed in about 30 minutes on a Pentium II Linux PC, and provides the time evolution of the resistance $R(t)$, along with the number of failed resistors per simulation cycle. In figure 3 $R(t)/R(0)$ is plotted for three different Monte Carlo runs until complete failure. The computed evolution of $R(t)$ is qualitatively very similar to the experimental behaviour: there is an initial phase in which the resistance increases linearly, until it is a few percent larger than the initial value, and a second phase in which the resistance increases in large and irregular steps until the catastrophic failure. While the initial phase is well reproducible among different Monte Carlo runs, the second phase exhibits large differences from run to run, and also the failure time has a very wide distribution.

It is very interesting to 'see' the formation of a void in a stripe. In figure 4 the snapshots of dissipated power density are plotted on a grey scale for the run of figure 3 which has the smallest failure time (thick line). A black dot corresponds to zero power density, while a white dot corresponds to maximum power density. Each snapshot is marked by the corresponding time instant T . As can be seen, in the initial phase failures occur at random in the stripe, exhibiting no particular correlation. Then, when a few adjacent failures occur, the currents flowing in the nearby resistors increase, and consequently their failure probabilities increase. At this point the second phase starts: the void enlarges at an increasing rate (note that the latest snapshots are much denser in time) until complete break-up of the stripe occurs. This behaviour is reproduced in all Monte Carlo runs, while the position of the critical void depends on the particular run.

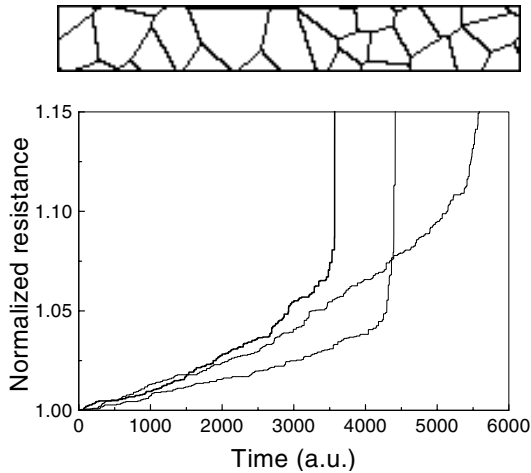


Figure 3. Grain pattern of the considered stripe (above) and stripe resistance as a function of time until complete failure for three different Monte Carlo simulations (below).

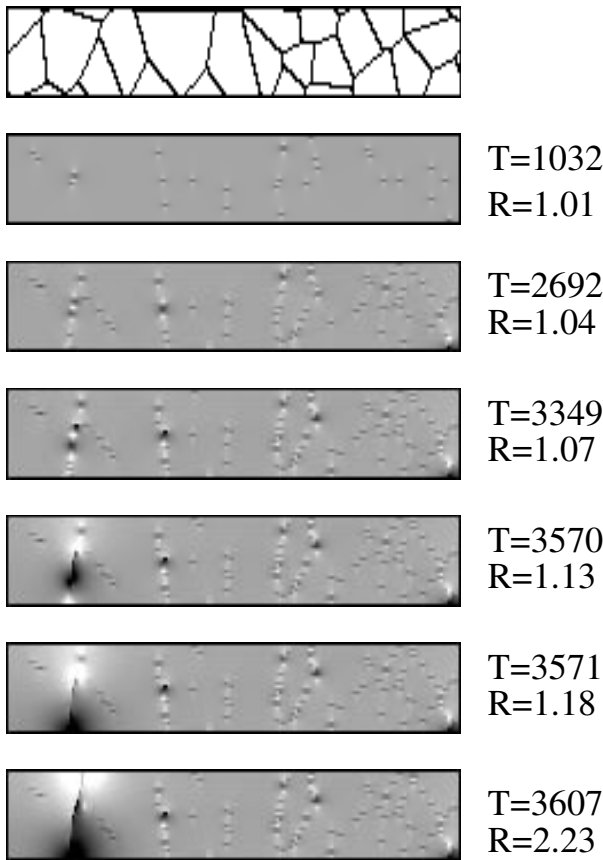


Figure 4. Snapshots of dissipated power density for the time evolution shown with a thick line in figure 3.

In order to reproduce the experimentally observed catastrophic behaviour, it is absolutely required to include a positive correlation between failures in adjacent resistors, because this mechanism causes the void growth. As we have said, we have done so by assigning to each resistor a failure probability exponentially dependent on the current. In this paper we will not address the problem of what is the particular physical mechanism leading to such an

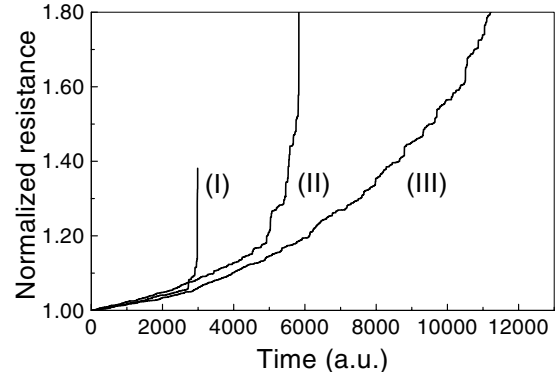


Figure 5. Time evolution of the normalized resistance of stripe shown in figure 3 for a failure probability depending on the current according to an exponential law (I), quadratic (II), linear (III).

expression; rather, we will justify our choice on the basis of phenomenological arguments, showing that smoother laws are not able to reproduce the time evolution of the stripe resistance observed in experiments. We have computed the time evolution of the stripe shown in figure 3 for three different relationships between the failure probability and the current density: (I) P_{fi} given by (1), (II) $P_{fi} = BI_i^2$, (III) $P_{fi} = CI_i$. The coefficients are chosen in order to have the same value of P_{fi} at time zero in all cases. The results of a single Monte Carlo run for each case are shown in figure 5.

As can be seen, a common evolution is observed for the three cases in the initial phase, when there are only a few failures and the values of P_{fi} are still very close to the initial ones. The evolution in the final phase, instead, is completely different: with the linear law (III) the correlation between adjacent failures is too weak, and the resistance increases almost linearly up to 130% of its initial value, and after then only slightly super-linearly. Even with the quadratic law (II) the $R(t)$ increases linearly up to $1.2 R(0)$, and then undergoes the steep increase that leads to the catastrophic failure. In experiments [2, 3, 11] the final failure is observed after an increase of only a few percent above $R(0)$, better reproduced by (1).

Since voids can only form and grow at grain boundaries, the grain size must play a major role in determining the damage rate and, consequently, the failure time. In our two-dimensional case, for given width and length of the stripe, the number of ‘boundary’ resistors—and therefore the initial damage rate—is inversely proportional to the square root of average grain area.

Figure 6 shows the results of three Monte Carlo runs for each of three different average grain sizes, i.e. average number of nodes N_G included in a single grain: (a) $N_G = 400$, (b) $N_G = 100$, (c) $N_G = 25$. The corresponding grain structures of the stripes are shown in figure 6 and are mapped onto a resistor network of 30×200 nodes. The initial phase of the evolution of $R(t)$ is rather reproducible for each type of stripe, and, as can be seen, the increase rate of $R(t)$ is roughly proportional to $1/\sqrt{N_G}$. Although only a small number of Monte Carlo runs are considered, it is apparent that the failure time increases with increasing grain size, as expected and known from experiments.

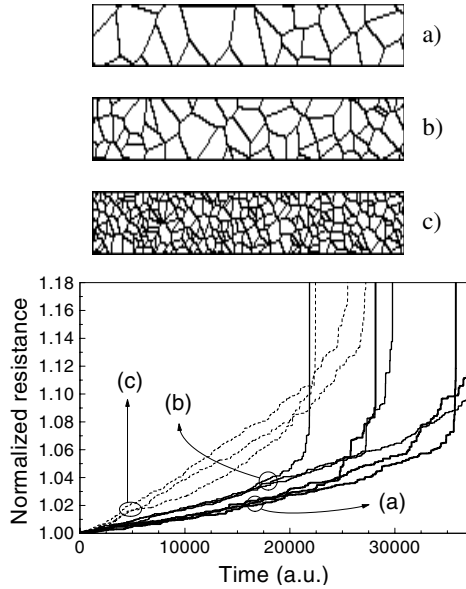


Figure 6. Stripe structures with three different average grain sizes (above) and normalized resistances as a function of time for three different Monte Carlo runs (below) for stripe (a) (thick lines), stripe (b) (thin lines), stripe (c) (dashed lines).

Additional information on this aspect can be obtained from the noise spectrum of $R(t)$ in the initial phase: it is well known from experiments [2, 3, 8, 11] that the spectral density of the noise associated with electromigration has a characteristic $1/f^\gamma$ behaviour. Experimental values of γ collected from 20 published papers are shown in table 1 of [8]: γ is found to be between 0.7 and 2.3. However, measurements at frequencies smaller than 1 Hz, which are able to better isolate fluctuations due to the electromigration process from other sources of noise [8], consistently yield a value of γ close to 2.

Since the resistance $R(t)$, on average, increases linearly with time and we are interested only in the spectrum of fluctuations, we first obtain $R_N(t)$ by subtracting from $R(t)$ the least squares fitting line, and then compute the power spectral density $S_{RN}(f)$ of R_N .

Figure 7 shows the average resistance noise spectra obtained from the Monte Carlo runs of figure 6 (each average is performed over the three runs corresponding to the same stripe). The plots are translated vertically in order to avoid overlap: actually, for a given frequency the noise power spectral density is roughly proportional to $1/\sqrt{N_G}$, as expected. In all cases $S_{RN}(f) \propto 1/f^\gamma$, with gamma between 1.96 and 2.

The noise spectrum is strongly dependent on the stripe width: in narrower stripes, a single failure leads to a larger increase in the total resistance. Figure 8 shows the noise spectra obtained from stripes with different widths: (a) is represented by a network of 90×200 nodes, (b) by a network of 30×200 nodes, (c) by a network of 10×200 nodes. For all three samples the grain average area was set to 100 nodes, corresponding to an equivalent diameter of 11 nodes. The resistance noise spectra are averaged from three different Monte Carlo runs. The γ exponents obtained from a least squares linear fit on the logarithmic scale are, again, between 1.96 and 2.

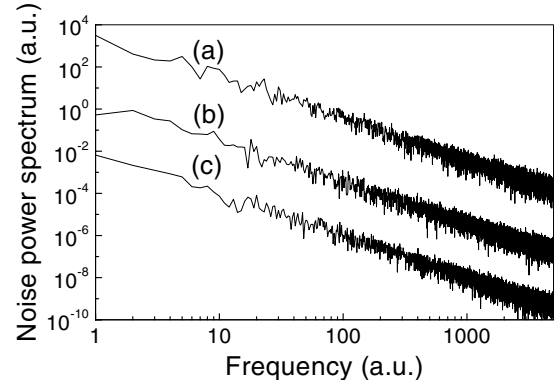


Figure 7. Electromigration noise spectra for the resistance evolutions shown in figure 6 averaged over the three different Monte Carlo runs (translated for clarity).

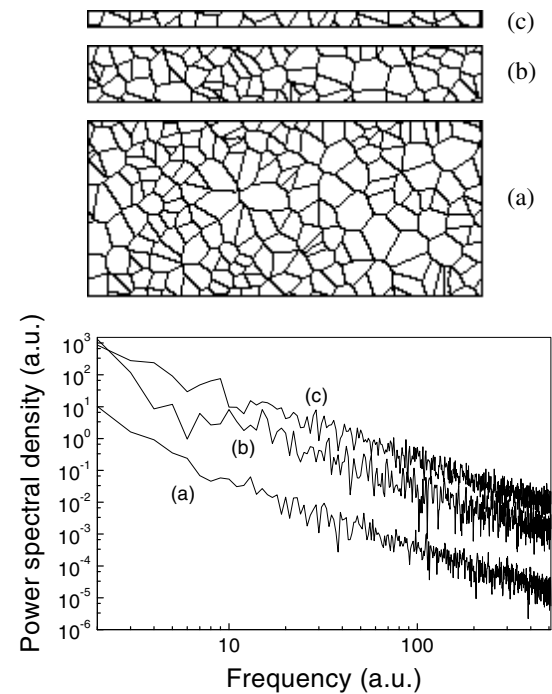


Figure 8. Stripe structures with three different widths and corresponding noise spectra averaged over three Monte Carlo runs.

The total noise power in the initial phase of linear resistance increase is roughly proportional to the inverse cube of the stripe width: the product $P_N W^3$, where P_N is the noise power and W the stripe width, is equal, in arbitrary units, to 0.178, 0.226 and 0.28 for a width of 10, 30 and 90 nodes, respectively.

To better investigate the effects of increasing damage of the stripes on electromigration noise a time dependent analysis of γ and of the noise power has been carried out. At time t , the mean noise power and the γ exponent are extracted from a portion of $R(t)$ in the time interval $(t, t + \Delta t)$. In this case the least squares fitting line of $R(t)$ is computed for each considered time interval and subtracted from $R(t)$ before the spectrum S_{RN} is computed. Since we are interested also in the behaviour up to the complete failure, the calculation has been performed on a single simulation run (in particular the one shown in figure 3 associated with the smallest failure time).

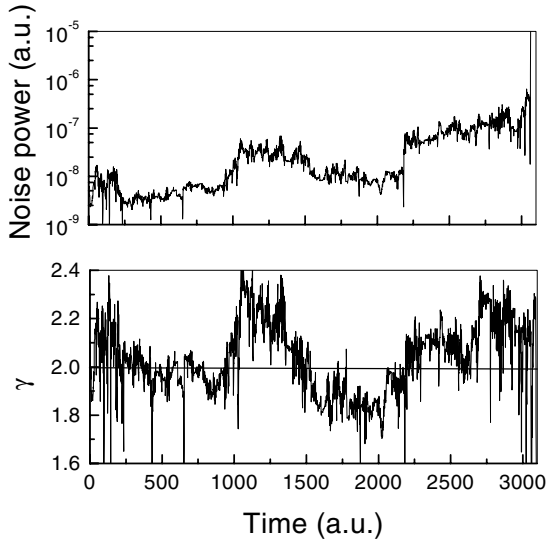


Figure 9. Noise power (above) and γ (below) as a function of time for the Monte Carlo run of figure 3 shown with the thick line.

As can be seen in figure 9, the exponent γ shows random fluctuations around 2 during the linear increase phase of the evolution of $R(t)$, while it approaches the value of 2.3 near the complete failure. On the other hand, the noise power exhibits a small average increase with time even in the initial phase, while in the final phase the increasing rate accelerates and leads to a noise power roughly two orders of magnitude larger than the initial one. Since the calculation has been performed on a single simulation run, the behaviour of γ and of P_N is very irregular, but is qualitatively reproducible among different Monte Carlo runs and similar to what has been observed in experiments [11].

4. Discussion

A very simple model can be used to derive the $1/f^2$ behaviour of the spectrum. Let us consider the function $y(t) = dR(t)/dt$: it can be written as a series of delta functions

$$y(t) = \sum_i \Delta R_i \delta(t - t_i) \quad (2)$$

where t_i is the instant at which the i th event (failure or repair) occurs, and ΔR_i is the corresponding change in the total resistance. If the individual events are independent, $y(t)$ is the result of a Poissonian process with probability per unit time λ [10], therefore the average of $y(t)$ is $\langle y \rangle = \lambda \langle \Delta R \rangle$ and its noise spectral density is

$$S_y(\omega) = 2\lambda \langle \Delta R^2 \rangle. \quad (3)$$

Since $R_N(t)$ is the time integral of the ac part of $y(t)$, its noise spectral density $S_{RN}(f)$ is

$$S_{RN}(\omega) = \frac{S_y(\omega)}{\omega^2} = \frac{2\lambda \langle \Delta R^2 \rangle}{\omega^2} \quad (4)$$

i.e. exhibits the $1/f^2$ behaviour. From (4) it can be seen that S_{RN} is roughly proportional to W^{-3} : λ is approximately proportional to the total number of resistors, therefore to W ; on the other hand ΔR is roughly proportional to W^{-2} in the initial phase when very few failures have occurred.

If there is some weak positive correlation between successive failures, the spectrum of $y(t)$ should be somewhat enhanced with respect to that of (3), the failure process being super-Poissonian. However, $S_y(\omega)$ would still be independent from frequency and therefore S_{RN} would still have an exponent γ equal to 2. The case of strong positive correlation, which is likely to occur near the complete failure, is different and needs deeper investigation.

5. Conclusion

We have shown that the simulation model proposed allows us to recover most of the characteristic features of the electromigration process measured experimentally, in particular, the initial linear increase followed by the irregular behaviour leading to the catastrophic failure, the dependence upon grain size and the noise spectrum. Even if the detailed physical mechanism for ion diffusion and void growth is not considered, we are confident in the fact that at a higher level the physics of the collective mechanism leading to the catastrophic failure is correctly included. Other important data, such as the mean failure time and its dependence on the stripe parameters, can be obtained as a result of simulations performed on statistically meaningful samples.

Acknowledgments

This work has been supported by the Ministry of Scientific and Technological Research of Italy and by the Italian National Research Council (CNR) through the project MADESS II.

References

- [1] Scorzoni A, Neri B, Caprile C and Fantini F 1991 *Mater. Sci. Rep.* **7** 143–220. This review contains several references to experimental work on the subject.
- [2] Neri B, Diligenti A and Bagnoli P E 1987 *IEEE Trans. Electron Devices* **34** 2317–22
- [3] Diligenti A, Neri B, Nannini A and Ciucci S 1991 *J. Electron. Mater.* **20** 559–65
- [4] Marcoux P J, Merchant P P, Naroditsky V and Rehder W D 1989 *Hewlett-Packard J.* **40** 79–84
- [5] Wu K and Bradley R M 1994 *Phys. Rev. B* **50** 12 468–87
- [6] Ciofi C and Di Pascoli S 1997 *Microelectron. Reliab.* **37** 77–85
- [7] Gungor R and Maroudas D 1998 *Appl. Phys. Lett.* **72** 3452–4
- [8] Neri B, Ciofi C and Dattilo D 1997 *IEEE Trans. Electron Devices* **44** 1454–9
- [9] Press W H, Teukolsky S A, Vetterling W T and Flannery B P 1992 *Numerical Recipes in Fortran 77* (Cambridge: Cambridge University Press)
- [10] van der Ziel A 1986 *Noise in Solid State Devices and Circuits* (New York: Wiley)
- [11] Ciofi C, Dattilo V and Neri B 1999 *Proc. IPFA99 (Singapore)*